Wetlands (2024) 44:122
https://doi.org/10.1007/s13157-024-01881-w

ORIGINAL RESEARCH ARTICLE

Modeling the Responses of Blue Carbon Fluxes in Mississippi River Deltaic Plain Brackish Marshes to Climate Change Induced Hydrologic Conditions

Hongqing Wang[1] · Ken W. Krauss[2] · Zhaohua Dai[3,4] · Gregory B. Noe[5] · Carl C. Trettin[3]

Received: 18 July 2024 / Accepted: 12 November 2024 / Published online: 23 November 2024

Abstract

Carbon fluxes in tidal brackish marshes play a critical role in determining coastal wetland carbon sequestration and storage, thus affecting carbon crediting of coastal wetland restoration. In this study, a process-driven wetland biogeochemistry model, Wetland Carbon Assessment Tool DeNitrification-DeComposition was applied to nine brackish marsh sites in Mississippi River (MR) Deltaic Plain to examine the responses of gross primary productivity (GPP), ecosystem respiration (ER), net ecosystem exchange (NEE), and emissions of methane (CH_4) and nitrous oxide (N_2O) to climate change. Simulations of a normal hydrologic year (2013), dry year (2011) and wet year (2021), and a hypothetical sea level rise (SLR) case were conducted as climate change scenarios. These climate change scenarios were determined by the Palmer Drought Severity Index (PDSI) for the Northeast Division of Coastal Louisiana during 2001–2021. Model results showed that GPP, ER, NEE, CH_4, and N_2O vary with site, and these brackish marshes lost carbon (net CO_2 emission) due to large reduction in primary productivity under the climate scenarios, as well as even during the normal hydrologic year. Average cross-site NEE were 148, 140 and 132 g C m^{-2} yr^{-1} in the dry, wet, and normal years (all net loss of wetland C). Under the hypothetical SLR, NEE were reduced by -25% compared to the normal year, but GPP and NPP were declined by -40% and -70%, respectively. These results suggest that climate change induced changes in soil salinity and water table depth will exacerbate carbon loss from tidal brackish marshes.

Keywords Blue carbon · Brackish marsh · Wetland Carbon Assessment Tool—DeNitrification-DeComposition (WCAT-DNDC) · Inundation · Drought

Introduction

Tidal (coastal) wetlands are situated between terrestrial and marine ecosystems, and include tidal freshwater forests (swamps), freshwater marshes, brackish marshes, salt marshes, mangroves, and seagrasses. Tidal wetlands are blue carbon ecosystems (Krauss et al. 2018; Adame et al. 2024). They are critical carbon sinks and store a disproportional amount of carbon (16–33% of terrestrial soil carbon pool with only about 3% of the Earth's surface) (e.g., Bridgham et al. 2006). However, tidal wetlands especially freshwater wetlands (forests and marshes) also emit 1/3 of the methane (CH_4) among all ecosystem types (Bridgham et al. 2006). The Global Carbon Project analyzed the Global Methane Budget 2000–2017 and found that CH_4 emissions from natural wetlands (excluding lakes, ponds, and rivers) are nearly 135 (116–155) TgCH_4 yr^{-1}, representing 30% on average of the global methane emissions (Saunois et al. 2020).

✉ Hongqing Wang
wangh@usgs.gov

1 U.S. Geological Survey, Wetland and Aquatic Research Center, Baton Rouge, LA 70810, USA

2 U.S. Geological Survey, Wetland and Aquatic Research Center, Lafayette, LA 70506, USA

3 USDA Forest Service, Center for Forested Wetlands Research, Cordesville, SC 29434, USA

4 College of Forest Resources and Environmental Science, Michigan Technological University, Houghton, MI 49931, USA

5 Florence Bascom Geoscience Center, U.S. Geological Survey, Reston, VA 20192, USA

Meanwhile, tidal wetland loss occurs due to sea level rise (SLR), increased storms, and human disturbances, releasing a large amount of carbon dioxide (CO_2) to the atmosphere through that mechanism rather than absorbing CO_2 from the atmosphere (Neubauer and Megonigal 2015). Globally, at least 13,700 km^{-2} of tidal wetlands have been lost, offset by gains of 9,700 km^{-2}, leading to a net loss of 4,000 km^{-2} from 1999 to 2019 (Murray et al. 2022). Additionally, tidal wetlands could also release nitrous oxide (N_2O), which is greenhouse gas with global warming potential of 298 times of that of CO_2 in a 100-year scale (e.g., Neubauer and Megonigal 2015). Net emissions of CH_4, CO_2, and N_2O to the atmosphere from tidal wetlands due to wetland loss and degradation reduce tidal wetland's capacity as carbon sinks to mitigate climate change impacts (e.g., Lane et al. 2016).

Carbon fluxes and pools along the atmosphere-plant-soil continuum in tidal wetlands vary spatially and temporally across landscapes with different vegetation community types (e.g., freshwater, brackish, and saline marshes) corresponding to a salinity gradient (Nyman and DeLaune 1991; Weston et al. 2014; Wilson et al. 2015; Li et al. 2020; Ishtiag et al. 2022). However, there are few studies that examine the spatial variability in carbon dynamics (fluxes and stocks) in the same vegetation type, especially for deteriorating brackish marshes (Krauss et al. 2016; Lane et al. 2016; Stagg et al. 2024). More studies can be found for tidal freshwater forests, freshwater marshes, and salt marshes (e.g., Krauss et al. 2018; Wang et al. 2022, 2023a). Tidal brackish marshes are normally low salinity wetlands with surface water salinity ranging from oligohaline (0. 5 to 5) to mesohaline (5 to 18 psu) (Russell et al. 2023; Adame et al. 2024). Soil porewater salinity in brackish marshes could be much higher than surface water salinity because of salt accumulation in soils via plant evapotranspiration (Wang et al. 2020; Russell et al. 2023). It was observed that soil salinity in brackish marshes along the Gulf of Mexico coast ranged from 4 to 25 psu (Snedden 2018; CPRA 2024).

Brackish marshes dominate global tidal marsh extents (Russell et al. 2023). Along coastal Louisiana, brackish (5–20 psu) marshes in 2013 and 2021 occupied 27.5% (Sasser et al. 2014) and 15.6% (Nyman et al. 2022) of total tidal marsh (freshwater, intermediate, brackish, and saline) area, respectively, and is a crucial component of tidal wetland carbon sequestration and storage when vegetation is healthy and productive. However, deteriorating brackish marsh could be a significant contributor to carbon loss via emissions of CO_2 and CH_4 and export of dissolved organic and inorganic carbon (Holm et al. 2016; Lane et al. 2016; Krauss et al. 2016; Russell et al. 2023). For example, Lane et al. (2016) found that brackish marshes in coastal Louisiana could emit 2.8 million tons (Mt) CO_2-eq ac^{-1} yr^{-1} to the atmosphere when vegetation dies, higher than that of salt marsh (2.07 Mt CO_2-eq ac^{-1} yr^{-1}). Drought, inundation, and increased salinity generally induce physiological stress in vascular plants thus affecting the biogeochemical processes in tidal wetlands (Janousek and Mayo 2013; Luo et al. 2019; Ishtiag et al. 2022; Wang et al. 2022, 2023a, b). Net ecosystem CO_2 exchange decreased from freshwater marsh to oligohaline marsh to mesohaline marsh with SLR-induced prolonged flooding and saltwater intrusion due to a greater decrease in gross primary production relative to ecosystem respiration, leading to the reduction in net CO_2 uptake (Li et al. 2020). Even within the same vegetation type, tidal wetlands could respond differently to climate change and SLR, resulting in varying carbon uptake and sequestration capacities, thus affecting net ecosystem exchange (NEE), or rather the net uptake versus net emission of CO_2 to the atmosphere (Bansal et al. 2023). Past studies on carbon and GHG fluxes in brackish marshes showed that the responses and mechanisms of NEE, gross primary productivity (GPP), ecosystem respiration (ER), CH_4 and N_2O fluxes in brackish marshes to changes in salinity, water table depth, or both could be variable with different magnitude and change direction. Outcomes of ecosystem change of CO_2 at coastal brackish marshes could be net uptake or net release of CO_2 under drought, flooding, and SLR. For example, little effect of elevated salinity on CO_2 uptake was found for a Florida Everglades brackish marsh when the site was inundated, but the site shifted from a C sink to a C source when water levels receded below soil surface (Wilson et al. 2018a). NEE measurements in a brackish marsh in the Florida Coastal Everglades indicated a net source of CO_2 due to the coupled effect of reduced photosynthesis suppressed by elevated salinity from 10 to 20 psu, thus substantially reduced both above- and below-ground NPP and increased ER (Ishtiag et al. 2022). Studies using greenhouse experiments and field mesocosms found that shoot production and biomass of brackish marsh species tended to decline monotonically with higher salinity and root production tended to be negatively affected by greater inundation under inundation and salinity stress especially for below-ground production (Janousek and Mayo 2013; Janousek et al. 2020; Ishtiag et al. 2022). Other studies found that the decreased net uptake of CO_2, or increase in net CO_2 release could be attributed to reduced GPP with no change in ER (Russell et al. 2023), both decreased GPP and ER, but greater decrease in GPP than ER (Li et al. 2020). CH_4 emissions tended to be reduced with increasing salinity in tidal marshes even within same marsh type with a salinity gradient (e.g., Poffenbarger et al. 2011). CH_4 efflux was considerably low (−0.3 to 2.3 g C m^{-2} yr^{-1}) with the increase of salinity from 10 to 20 psu at a brackish marsh site in the Florida Coastal Everglades (Ishtiag et al. 2022). However, CH_4 flux was found to be relatively small with no significant differences across sites with different salinities in the Mobile Bay marshes along the Northern Gulf of Mexico (freshwater: 2.3 psu, brackish: 5.1 psu, and saline: 20.7 psu) due to a significant quantity of CH_4 oxidation occurs at the sediment-atmosphere interface of the lower salinity site (Wilson et al. 2015). Elevated salinity was found to have no effect on CH_4 efflux in an experiment using sawgrass (*Cladium jamaicense*) and soil collected from Everglades brackish marshes (Wilson et al. 2018a). In contrast, saltwater intrusion resulted in large effluxes of CH_4 (80 g C-CH_4 m^{-2} yr^{-1}) at the oligohaline marsh site (~5.6 psu) in Delaware River Estuary, thus a large but likely localized source of GHG (2,000 g CO_2-eq m^{-2} yr^{-1}) to the atmosphere (Weston et al. 2014).

The spatial and temporal variations in carbon fluxes and the different responses to climate change and SLR within a vegetation type are determined by variations in marsh elevation and soil properties (e.g., bulk density, organic matter content, total nitrogen). Such elevation and soil variability control the input of tidal water and freshwater with varying frequency, duration, and intensity and various salinity, mineral sediment, and nutrients into coastal wetlands. These various inputs of water, sediment, and nutrients cause changes in ecological (e.g., plant productivity, soil organic matter decomposition, sulfate reduction, methanogenesis, nitrification, denitrification) and physical (e.g., sediment transport, deposition, and erosion) processes, resulting in different carbon fluxes over space (Poffenbarger et al. 2011; Wilson et al. 2015; Wang et al. 2022, 2023a). Nevertheless, there are very few studies that examine the spatial responses of coastal brackish marshes in the context of NEE, GPP, ER, CH_4 and N_2O under climate change and rising sea level.

The Wetland Carbon Assessment Tool (WCAT)-DeNitrification-DeComposition (DNDC) is a process-based simulation model of water, carbon (C), nitrogen (N) and phosphorus (P) biogeochemistry in wetland ecosystems. WCAT-DNDC was developed for a wide range of wetlands with and without tidal influence such as freshwater swamp forest, freshwater marshes (< 0.5 psu), and oligohaline marshes (< 5 psu), to high salinity wetlands such saline marshes (> 18 psu) and mangrove forests. WCAT-DNDC was calibrated and validated by field observations on carbon fluxes including plant primary productivity, soil organic matter decomposition, emissions of CH_4 and N_2O at tidal and nontidal freshwater forests, oligohaline marshes (Zhang et al. 2002; Dai et al. 2012; Wang et al. 2022, 2023a) and mangroves (Dai et al. 2018). Application of wetland biogeochemistry models such as WCAT-DNDC can help wetland ecologists determine the spatial variability in tidal wetland carbon sequestration and carbon loss and assess the impacts of climate change-induced inundation, drought, and SLR on carbon fluxes with limited field monitoring data at few sites. The objectives of present study are to 1) validate WCAT-DNDC using field carbon flux data for application in tidal brackish marshes having the same or similar plant species composition and soil salinity in the range of 5–25 psu; 2) determine the spatial variability in GPP, ER, GHG emissions and NEE in tidal brackish marshes; and 3) examine the impact of marsh inundation, drought and SLR on GPP, ER, GHG emission and NEE. Results of this modeling study may help coastal resource managers to design tidal brackish marsh restoration projects that enhance project carbon credit capture via promoting net carbon uptake and reducing net CO_2 emission compared to a no-action scenario.

Methods

Study Sites

Nine brackish marsh sites (Fig. 1) within the Terrebonne Basin, Louisiana, along the Northern Gulf of Mexico coast were selected from the Coastwide Reference Monitoring System (CRMS, http://lacoast.gov/crms2/home.aspx). Terrebonne Basin is an inactive basin of Mississippi River Deltaic Plain (MRDP) with separation from riverine sedimentation (Cassaway et al. 2024; Stagg et al. 2024). These brackish marsh sites are adjacent to Pointe-aux-Chenes Wildlife Management Area (WMA) managed by Louisiana Department of Wildlife and Fisheries (LDWF). These sites were all classified as brackish marsh except CRMS3296 that was classified as salt marsh during 2011–2013, reflecting rapid habitat change in coastal Louisiana. CRMS3296 was selected since it was in the transition zone between brackish and salt marshes and used to be a brackish marsh site during late 1980s and early 1990s. CRMS2825 was selected because it was the only existing brackish marsh site that had carbon flux data from both the eddy covariance (EC) technique and static chamber method (Holm et al. 2016; Krauss et al. 2016). Marsh surface elevation, excluding CRMS0312 which is a floating marsh, ranged between 0.24 and 0.85 m North American Vertical Datum of 1988 (NAVD88) (Table 1). Using the 1 km × 1 km landscape unit, land (emergent vegetation, upland, wetland forest, or scrub-shrub) and water (open water, aquatic beds, and mudflats) area and percentage for all CRMS sites including the selected brackish marsh sites were determined with high resolution (1 m) digital aerial photography. Land percentage (vs. water) in 2012 of these brackish marshes ranged from 30.4% (CRMS3296) to 88.7% (CRMS0312) (Table 1). These brackish marsh sites are microtidal with a range < 0.3 m diurnal (Krauss et al. 2016). Mean surface water salinity ranged from 3.5 practical salinity units (psu) (oligohaline: 0.5–5 psu) at CRMS0385 [the other site with < 5 psu is CRMS0312)] to 13.1 psu (mesohaline: 5–18 psu) at CRMS3296 (Table 1). Mean water levels at these marsh sites (2006–2013) were similar, ranging between 0.3 and 0.45 m NAVD88 (Table 1). Dominant plant species include *Spartina patens* except CRMS0400 dominated by *Schoenoplectus americanus* and CRMS3296

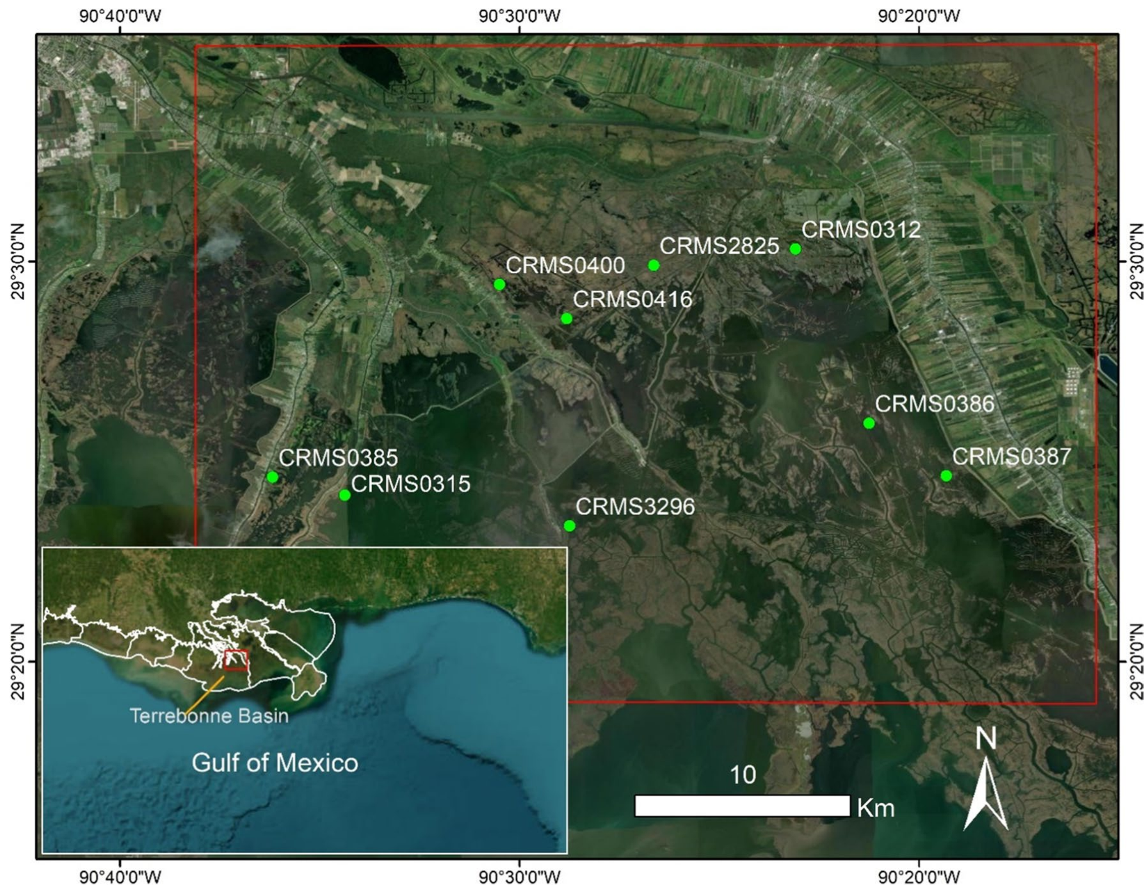

Fig. 1 Map of coastal zones and the Coastwide Reference Monitoring System (CRMS) brackish marsh sites in the Terrebonne Bay, Louisiana. Source of imagery: World Imagery, ArcGIS Online Basemap, Esri

Table 1 The geomorphologic, hydrologic, and soil characteristic in the brackish marsh sites from the Coastwide Reference Monitoring System (CRMS)

Characteristic	CRMS0385	CRMS0400	CRMS0312	CRMS0315	CRMS2825	CRMS0386	CRMS3296	CRMS0416	CRMS0387
Latitude (°N)	29.4107	29.4906	29.5051	29.4035	29.4978	29.4325	29.3890	29.4761	29.4107
Longitude (°W)	90.6043	90.5105	90.3855	90.5730	90.4480	90.3543	90.4793	90.4793	90.3230
Elevation (m, NAVD88)	0.00	0.11	floating	0.17	0.18	0.08	0.13	0.14	0.05
2012 Land %	74.60	75.80	88.70	30.90	83.70	39.90	30.40	55.10	48.10
Mean water salinity (psu, record period)	3.51 (10/2012-2/2023)	5.51 (2/2006-1/2023)	3.6 (5/2006-8/2021)	8.97 (6/2006-2/2023)	5.58 (3/2008-1/2023)	11.25 (6/2006-1/2023)	13.13 (5/2009-2/2023)	7.19 (6/2006-1/2023)	12.79 (5/2006-2/2023)
Mean water level (m, NAVD88, record period)	0.37 (9/2012-9/2013)	0.45 (9/2006-9/2013)	0.36 (9/2006-9/2013)	0.43 (9/2006-9/2013)	0.35 (9/2008-9/2013)	0.36 (9/2006-9/2013)	0.43 (9/2009-9/2013)	0.39 (9/2006-9/2013)	0.30 (9/2006-9/2013)
Soil organic matter (%)	42.81	58.84	84.50	26.12	58.30	56.50	38.59	56.65	52.30
Soil bulk density (g cm^{-3})	0.19	0.09	0.08	0.26	0.14	0.14	0.23	0.13	0.12

dominated by *Spartina alterniflora*. Soils at these brackish marsh sites are generally organic with lowest organic matter content (26.12%) and highest bulk density (0.26 g cm^{-3}) at CRMS0315 and highest organic matter content (84.5%) and lowest bulk density (0.08 g cm^{-3}) at CRMS0312 (Table 1). Soil organic carbon content varied among these brackish marsh sites ranging from 0.09 (kg C kg^{-1}) at CRMS3296 to 0.40 kg C kg^{-1} at CRMS0312 (Table 1).

Wetland Carbon Assessment Tool

WCAT-DNDC consists of five sub-models: hydrology, plant growth, soil organic matter, methanogenesis/methanotroph activity, and nitrification/denitrification (Fig. 2). The drivers of WCAT-DNDC include climate, hydrology, soil, vegetation, and disturbance. WCAT-DNDC incorporates critical biogeochemical processes including photosynthesis, plant and soil respiration, soil organic matter decomposition, N/P mineralization, methanogenesis, methanotrophy, nitrification, denitrification, carbon allocation, storage, and consumption. The impacts of environmental factors such as soil salinity, water level or water table depth, light/radiation, air/soil temperature, precipitation, soil moisture, redox potential, soil pH, and nutrients on these biogeochemical transformations are included in WCAT-DNDC. There are very few process-based biogeochemistry models that can simulate water, carbon, nitrogen, and phosphorus dynamics in saline environment. WCAT-DNDC evolved from MCAT-DNDC for mangroves (Dai et al. 2018) and TFW-DNDC for low salinity forested wetlands including tidal freshwater swamps and marshes (Wang et al. 2022, 2023a). In addition to the impact of water level and nutrient (N, P, S) on C, N, P biogeochemical processes, salt stress on coastal wetland processes such as primary productivity, soil organ matter decomposition and GHG emissions has been successfully incorporated in WCAT-DNDC. Calibration, validation, and application of WCAT-DNDC have been conducted for mangroves (Dai et al. 2018), and tidal swamps and marshes (Wang et al. 2022; Wang et al. 2023a, b). For this study, the coastal marsh sub-model was recalibrated and validated using field data (see "Model validation and performance" section). The major ecosystem processes and model parameters in WCAT-DNDC are presented in Table S1 in Appendix S1 and Table S2 in Appendix S2 of Wang et al. (2022) as well as in Dai et al. (2018), Li et al. (2000), Li et al. (2004), and Zhang et al. (2002). To be

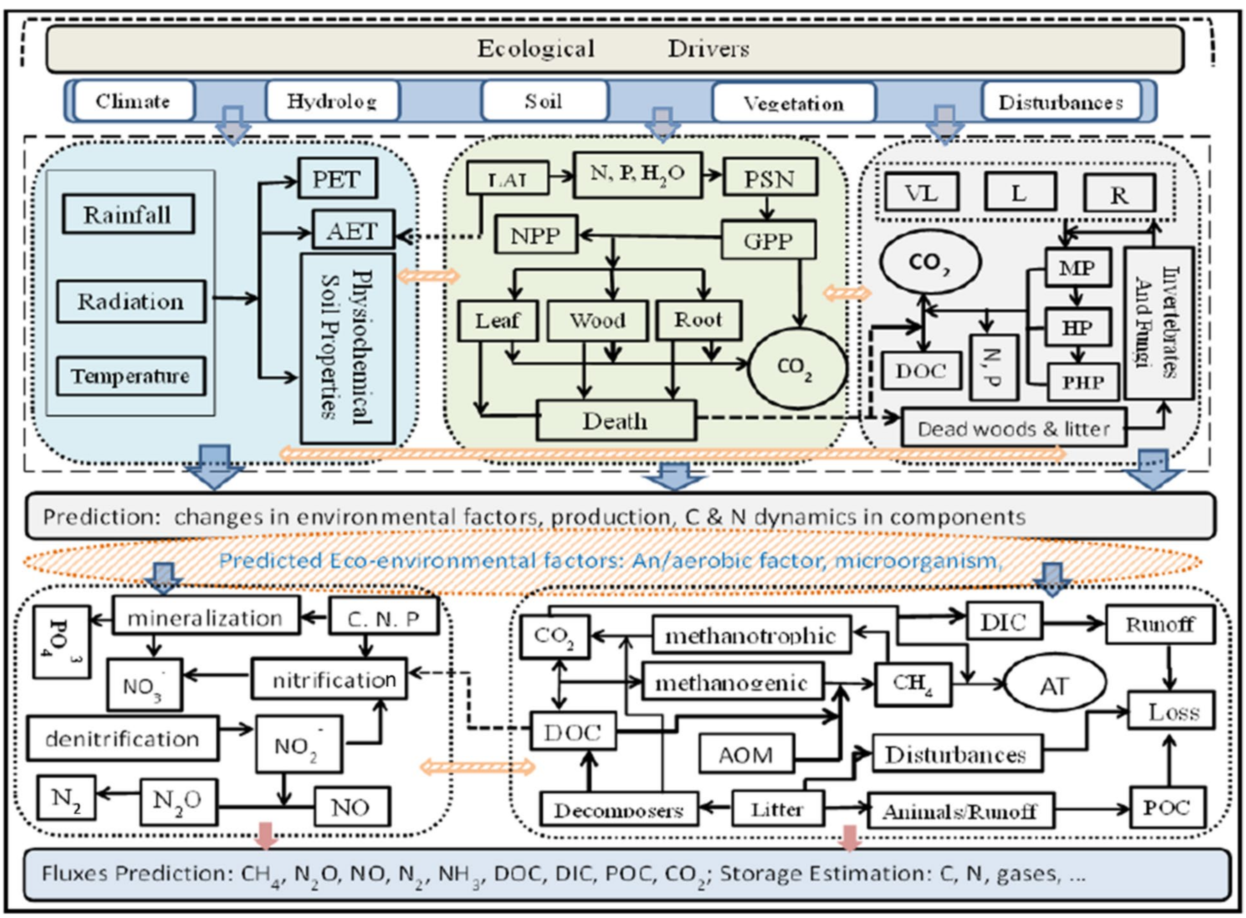

Fig. 2 The framework of Wetlands Carbon Assessment Tool—DNDC. WT: water table; Ra: radiation; PET: potential evapotranspiration; AET: estimated actual evapotranspiration; PSN: photosynthesis; NPP: net primary production; GPP: gross primary production; Death: including fallen leaf and dead woods; VL: very labile organic matter; L: labile organic matter; R: resistant organic matter; MP: mineral C pool; HP: humus pool; PHP: passive humus pool; DIC: dissolved inorganic C; DOC: dissolved organic C; AT: atmosphere; POC: particulate organic C; AOM: anaerobic oxidation of methane (modified from Dai et al. 2018)

effective in simulating carbon and GHG fluxes in brackish marshes (salinity: 5–18 psu), modification of WCAT-DNDC was done using data from brackish marshes along coastal Louisiana. Specifically, the impact of salinity on plant productivity of the brackish marshes was modified based on marsh organ experiment data for *S. patens* along coastal Louisiana (Snedden et al. 2015). The impact of salinity on CH_4 emission was modified based on the relationship (decreasing with increased salinity) found for brackish marshes (Holm et al. 2016). WCAT-DNDC is written in C/C++ and operates on a daily time step with summation to annual output. As with Wang et al. (2022), a spin up period of three years was adopted to reduce the influences of initial conditions (primarily soil salinity and water level) and numerical calculations on model stability. Soil depth in this study was simulated to 50 cm below the soil surface.

Model Input and Output

Input data include site-specific geographical location (latitude, longitude), elevation, vegetation, soil (Table 1), and time-series of climate indicators (daily precipitation, maximum and minimum temperature) and hydrology (soil salinity and soil water table depth). Daily temperature and rainfall at the brackish marsh sites were obtained from the Oak Ridge National Laboratory's Daily Surface Weather and Climatological Summaries (Daymet) database (Thornton et al. 2020). Data on daily soil water table depth at these brackish marsh sites were obtained from CRMS (CPRA 2024). Daily soil porewater salinities at the nine selected brackish marsh sites were simulated using a mass-balance-based soil salinity model, which was developed for tidal wetlands including salt marshes (Wang et al. 2007), and salinity impacted forested wetlands and oligohaline marshes (Wang et al. 2020). Input data for the soil salinity model include daily air temperature, hourly rainfall, incoming tidal elevation, and salinity. The soil salinity model for the brackish marshes was calibrated using 2011 CRMS field soil porewater data and validated using 2012 CRMS field data. Two sites, CRMS3296 and CRMS0387, were not validated since field data during 2011–2012 were not available. Comparisons between simulated and observed soil salinities with all data of the seven sites for calibration ($R^2=0.97$) and validation ($R^2=0.98$) showed that simulated soil salinities are in good agreement with observations capturing both the magnitude and seasonal pattern with high accuracy (Figs. S1 and S2). Output of WCAT-DNDC for this study include daily and annual rates of GPP, ER, NEE, CH_4 and N_2O. NEE was calculated via NEE = ER – GPP, therefore, positive values indicate net CO_2 emissions to the atmosphere while negative values indicate net CO_2 uptake.

Model Validation and Performance

Field data on daily GPP, ER, NEE, and CH_4 were collected from October 8, 2011 to December 5, 2012 at CRMS2825 using the EC technique (Holm et al. 2016; Krauss et al. 2016). Missing data on these carbon fluxes were gap-filled with an algorithm-derived procedure (Reichstein et al. 2005) and stepwise regression analysis using meteorological and environmental covariates. For details about EC-derived carbon fluxes, processing and uncertainty refer to Krauss et al. (2016). Observed data in 2011 were used for model calibration and data in 2012 were used for model validation. For daily NEE, there were no data during May 6 to June 24, 2012, and gap-filled data were not used for model comparison due to the large uncertainty for gap-filling a period with longer than one month. For other fluxes with few days of gaps, the gap-filled data were used for model validation.

The performance of WCAT-DNDC in simulating carbon dynamics and GHG emissions in MRDP brackish marshes was evaluated using the coefficient of determination (R^2), root mean square error (RMSE), and bias. The coefficient of determination measures the linear association between modeled and observed data; a high correlation coefficient is considered desirable. Typically values greater than 0.5 are considered acceptable. RMSE describes the residual difference between model performance and actual data; a good model has low RMSE values. Bias is the average of the difference between modeled and observed values; a good model exhibits low bias. Values for R^2, RMSE and Bias are calculated as:

$$R^2 = \left(\frac{\sum(O_i - \overline{O})(P_i - \overline{P})}{\sqrt{(O_i - \overline{O})^2}\sqrt{(P_i - \overline{P})^2}}\right)^2 \tag{1}$$

$$RMSE = \sqrt{\frac{\sum (P_i - O_i)^2}{n}} \tag{2}$$

$$Bias = \frac{\sum(P_i - O_i)}{n} \tag{3}$$

where O_i and P_i are observed and simulated values at each time *i;* $\overline{O}$ and $\overline{P}$ are observed mean and simulated mean; *n* is the number of observations.

Scenario Analysis

The validated WCAT-DNDC was used to examine trends and variability in carbon fluxes at the selected brackish marsh sites in MRDP under normal, flooding and drought conditions. Normal, wet, and dry years in this study were determined by the Palmer Drought Severity Index (PDSI) for the Northeast Division of Coastal Louisiana during 2001–2021. Year 2013 was determined to represent normal years, Year 2021 (third heaviest precipitation year on record) represents wet years, and Year 2011 represents dry years. The statistical summaries of soil salinity and water table depth are shown in Table 2. Under the normal year, averaged daily soil water table depth across sites was 26.7 cm, ranging from −3.2 cm (below soil surface) to 69.4 cm (above surface). Averaged daily soil salinity across sites was 8.2 psu, ranging from 3.4 to 12.4 psu. Under the wet year, averaged daily soil water table depth across sites was 35.5 cm, ranging from 12.7 cm to 51.5 cm (above surface). Averaged daily soil salinity across sites was 7.5 psu, ranging from 3.9 to 11.7 psu. Under the dry year, averaged daily soil water table depth across sites was 11.8 cm, ranging from −11 cm (below soil surface) to 33.6 cm (above surface). Averaged daily soil salinity across sites was 11.7 psu, ranging from 5.4 to 16.6 psu. Since the dry year did not represent increases in both soil salinity and water level, we added a hypothetical SLR case by using the soil salinity in the dry year and soil water table depth in the wet year. Climate data in the normal year was used for the SLR case. Soil water table depth increased in the range of 10 to 30 cm under the SLR case compared to the normal year at these sites (excluding CRMS0386 and CRMS0387). The upper increase (30 cm) corresponds approximately to a moderate SLR (27 cm) over the next 50 years and a less optimistic SLR (45 cm) over the 25 years for coastal Louisiana (Wang et al. 2017). We also conducted a numerical experiment with varying soil salinity (1.1 to 41.6 psu) and water table depth (2.5 ~ 128.6 cm) in relation to the SLR case to determine the threshold values of soil salinity and water level that would generate net C sequestration (NEE < 0, net uptake of CO_2).

Statistical Analysis

The impacts of flooding and drought on simulated daily carbon and GHG fluxes (NEE, GPP, ER, CH_4, N_2O) at the nine brackish marsh sites were analyzed using two-way ANOVA with site and scenario and their interaction as explanatory variables. When necessary, the simulation results were transformed using the Box-Cox method prior to analysis to meet normality and homoscedasticity assumptions. Whenever

Table 2 Statistical summary of the daily soil water table depth and soil salinity in dry year (2011), normal year (2013) and wet year (2021) at the brackish marsh sites along coastal Louisiana

Sites	Dry (2011)			Normal (2013)			Wet (2021)		
	Mean	Max	Min	Mean	Max	Min	Mean	Max	Min
	Water Table Depth (cm)								
CRMS0385	13.93	41.98	1.03	20.21	47.65	10.06	30.73	69.66	19.38
CRMS0400	15.90	89.13	-23.46	29.15	79.67	-13.75	39.74	108.00	-1.16
CRMS0312	-2.46	64.00	-31.39	3.28	40.82	-23.85	31.96	123.74	-18.79
CRMS0315	-10.98	88.25	-35.50	-1.01	67.54	-38.00	12.65	68.92	-47.82
CRMS2825	-7.39	72.17	-49.54	-3.17	28.54	-37.75	24.03	115.74	-26.79
CRMS0386	27.66	137.04	-22.46	40.54	103.71	-11.79	36.80	115.40	-15.62
CRMS3296	18.93	120.21	-31.75	34.10	103.46	-16.83	42.66	107.82	-11.67
CRMS0416	33.56	110.29	-5.08	48.17	98.71	6.71	49.51	121.40	3.18
CRMS0387	16.84	127.83	-32.54	69.40	137.50	18.88	51.48	128.40	5.51
	Salinity (psu)								
CRMS0385	10.31	12.50	7.31	7.02	7.27	6.92	7.95	8.79	7.30
CRMS0400	10.75	14.82	7.38	5.32	9.04	3.20	4.34	11.93	1.64
CRMS0312	5.38	8.46	3.90	3.40	5.00	2.25	3.91	6.10	2.56
CRMS0315	10.84	12.11	9.30	9.12	10.20	8.00	7.40	9.84	4.73
CRMS2825	10.08	10.72	9.38	8.35	9.35	7.33	7.69	9.41	6.37
CRMS0386	15.30	19.42	13.48	10.30	13.19	8.11	9.22	13.67	5.14
CRMS3296	16.63	19.79	14.69	12.37	15.78	9.76	11.69	15.55	7.96
CRMS0416	10.46	13.00	8.27	6.21	9.13	4.01	6.05	11.17	2.89
CRMS0387	15.85	20.51	11.77	11.55	14.46	9.44	9.61	13.29	5.67

a significant interaction effect was detected via two-way ANOVA, a series of one-way ANOVAs were used to analyze individually the impact of flooding, drought and the SLR case on carbon and GHG fluxes at each of the nine brackish marsh sites. The Tukey–Kramer post hoc test was used to compare the means between each pairwise combinations of the dry, normal, wet and SLR scenarios and determine if the differences are statistically significant. The SAS 9.3 software package (SAS Institute, Cary, North Carolina, USA) was used for the statistical analyses. All the tests were two-tailed based on type III sums of squares (SS) and considered significant at $p < 0.05$.

Results

Model Performance

WCAT-DNDC simulated daily NEE, GPP, ER, CH_4 and N_2O fluxes were within the ranges of EC-derived observations. Simulated NEE fluxes (mean ± standard deviation: 0.37 ± 0.27 g C m^{-2} day^{-1}) and seasonal variation agreed with observed fluxes (0.41 ± 0.49 g C m^{-2} day^{-1}) and seasonal variation ($R^2 = 0.35$, RMSE = 0.53 g C m^{-2} day^{-1}) although WCAT-DNDC tended to underpredict observed

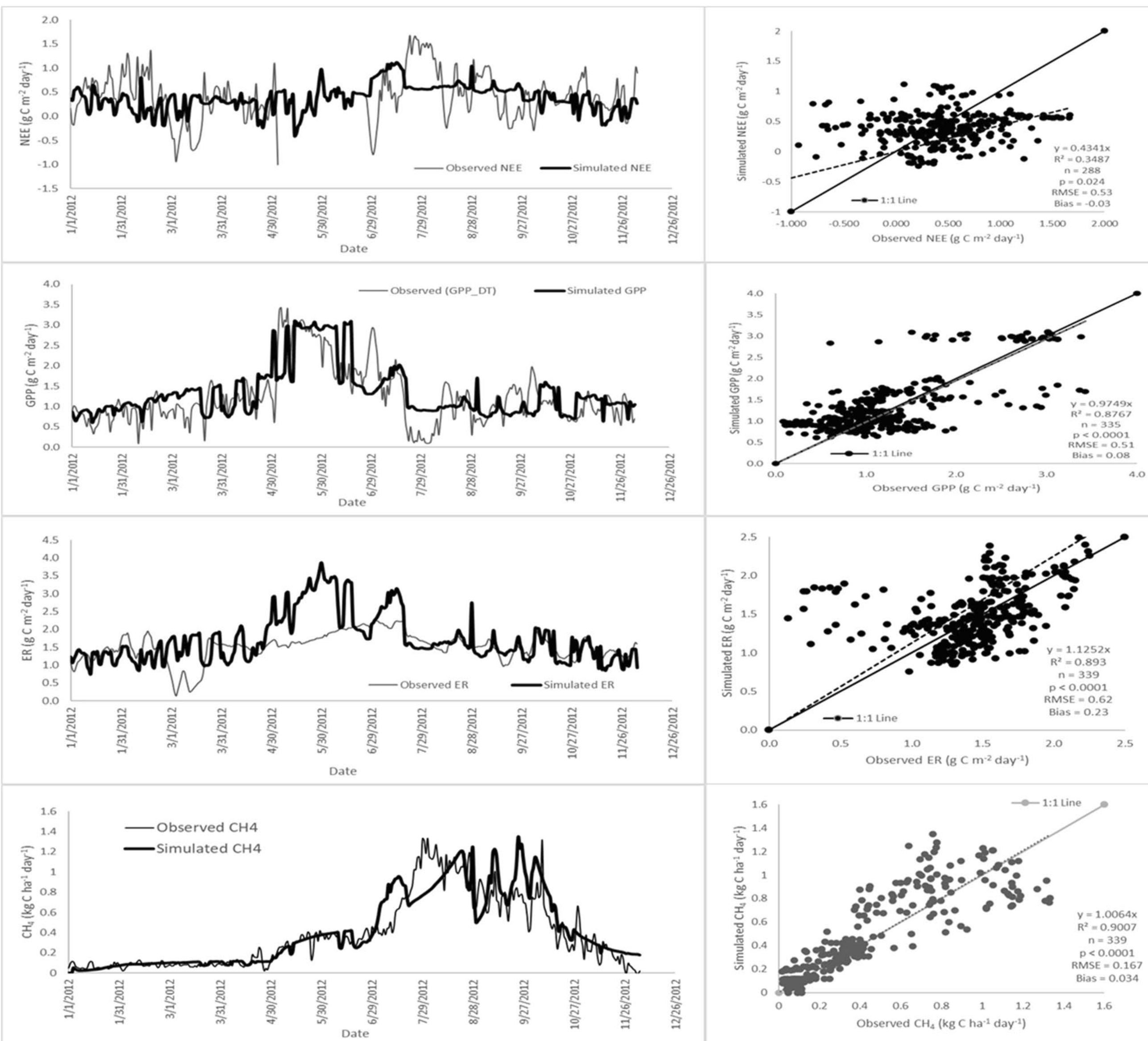

Fig. 3 Comparisons between simulated and observed net ecosystem exchange (NEE), gross primary productivity (GPP), ecosystem respiration (ER), and methane (CH_4) emissions at CRMS2825 in 2012. Observed NEE, GPP, ER and CH_4 emissions were from the eddy covariance (EC) technique

NEE (bias = −0.03 g C m^{-2} day^{-1}) (Fig. 3). Simulated daily GPP, ER, and CH_4 fluxes showed good agreements with EC-derived observations (R^2 and RMSE were 0.88 and 0.51 g C m^{-2} day^{-1} for GPP, 0.89 and 0.62 g C m^{-2} day^{-1} for ER, and 0.90 and 0.17 kg C ha^{-1} day^{-1} for CH_4, respectively), although the model tended to slightly overestimate GPP, ER and CH_4 fluxes (biases = 0.08 g C m^{-2} day^{-1}, 0.23 g C m^{-2} day^{-1}, and 0.03 kg C ha^{-1} day^{-1} for GPP, ER and CH_4 fluxes, respectively) (Fig. 3). The lower R^2 for NEE comparison than that of GPP and ER comparisons could be related to the missing and poor-quality data from the eddy covariance technique applied in coastal wetlands (e.g., Lu et al. 2024). There was a total of 80 days (22% of the year) of missing EC-derived NEE data from May 6 to September 3 in 2012, leading to the low accuracy in filled NEE data. WCAT-DNDC accurately captured the summer peak in observed GPP (simulated = 3.2 vs. observed = 3.4 g C m^{-2} day^{-1}) and peak in CH_4 in late summer to fall (simulated = 1.33 vs. observed = 1.34 kg C ha^{-1} day^{-1}) whereas the model captured seasonality in ER well (average fluxes: simulated = 1.68 vs. observed = 1.50 g C m^{-2} day^{-1}) except the summer ER (Fig. 3). Low observed and simulated GPP during July 20 and August 9, 2012 could be attributed to the higher temperature (> 33 °C) and higher rainfall accumulation (21 cm total and up to 12.5 cm day^{-1}) during that period, inhibiting plant photosynthesis. The discrepancies between observed and simulated ER in March, May and June could be attributed to the influence of wind speed and direction (Holm et al. 2016; Mayen et al. 2024) that are not incorporated in the simulations. Limited daily N_2O data (only five dates during March and October in 2012 from static flux chambers) were available for model validation. Simulated daily N_2O fluxes (mean = 3.32, range = 2.4 – 4.3 g N ha^{-1} day^{-1}) were within the observed fluxes (mean = 3.36, range = −4.0 – 13.0 g N ha^{-1} day^{-1}). Overall, model validation of selected attributes suggests that WCAT-DNDC represented the biogeochemical processes well and can simulate blue carbon fluxes in coastal brackish marshes effectively.

Spatial Variability in Carbon Fluxes and N_2O Emission

The two-way ANOVA result (Table S1) revealed that NEE, GPP, ER, CH_4 and N_2O fluxes differ significantly ($p < 0.0001$) by brackish marsh sites, suggesting spatial variability in these blue carbon wetland fluxes in tidal brackish marshes. Across the nine brackish marsh sites, annual GPP ranged 228 – 833 g C m^{-2} yr^{-1} (Fig. 4), ER ranged 332 – 1046 g C m^{-2} yr^{-1} (Fig. 5) and NEE ranged 104 – 213 g C m^{-2} yr^{-1} under the normal year (Fig. 5). Under the wet year, dry year and hypothetical SLR, annual GPP, ER and NEE were within the ranges of the normal year (Figs. 4 and 5). Highest GPP (832 g C m^{-2} yr^{-1}, normal year), ER (1104 g C m^{-2} yr^{-1}, dry year) and NEE (273 g C m^{-2} yr^{-1}, dry year) were found at the floating marsh CRMS0312 (Figs. 4, 5) where highest soil organic matter content (84.5%, Table 1) and lowest soil salinity (3.4 psu under the normal year, Table 2) were found among the nine brackish marsh sites. Although negative NEE values (net uptake of CO_2) occurred for daily NEE (e.g., Fig. 3), annual NEE fluxes were all positive, or lost from the ecosystem to the atmosphere for the four scenarios, indicating that all these brackish marshes lost carbon even under normal conditions. For GHG emissions across the brackish marshes, annual average CH_4 fluxes ranged 5.3 – 40.4, 6.2 – 28.2, and 2.1 – 34.0, and 0.9 – 17.4 g C m^{-1} yr^{-1} under the normal, wet, dry years and hypothetical SLR (Fig. 6). Annual N_2O fluxes ranged 1.7 – 5.0, 1.6 – 4.9, and 2.1 – 5.4, and 1.4 – 4.4 kg N ha^{-1} yr^{-1} under the normal, wet, dry years and hypothetical SLR (Fig. 6).

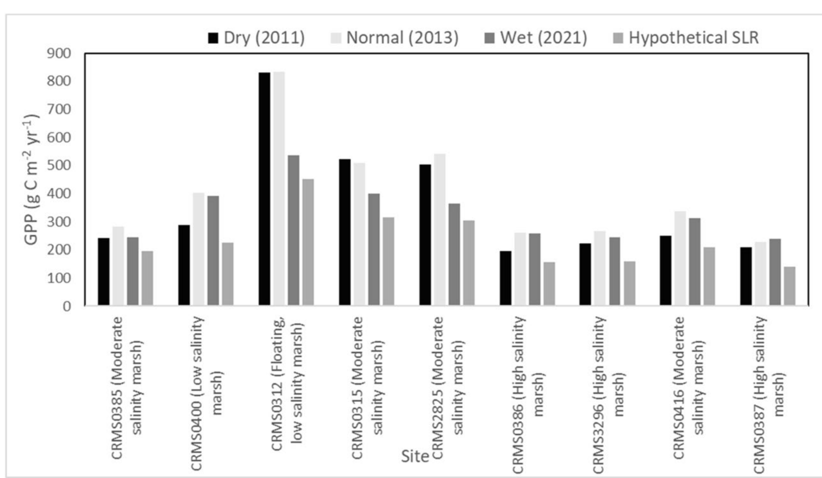

Fig. 4 Simulated GPP under the dry, normal, wet, and hypothetical SLR conditions in the brackish marsh sites in Terrebonne Basin, Louisiana

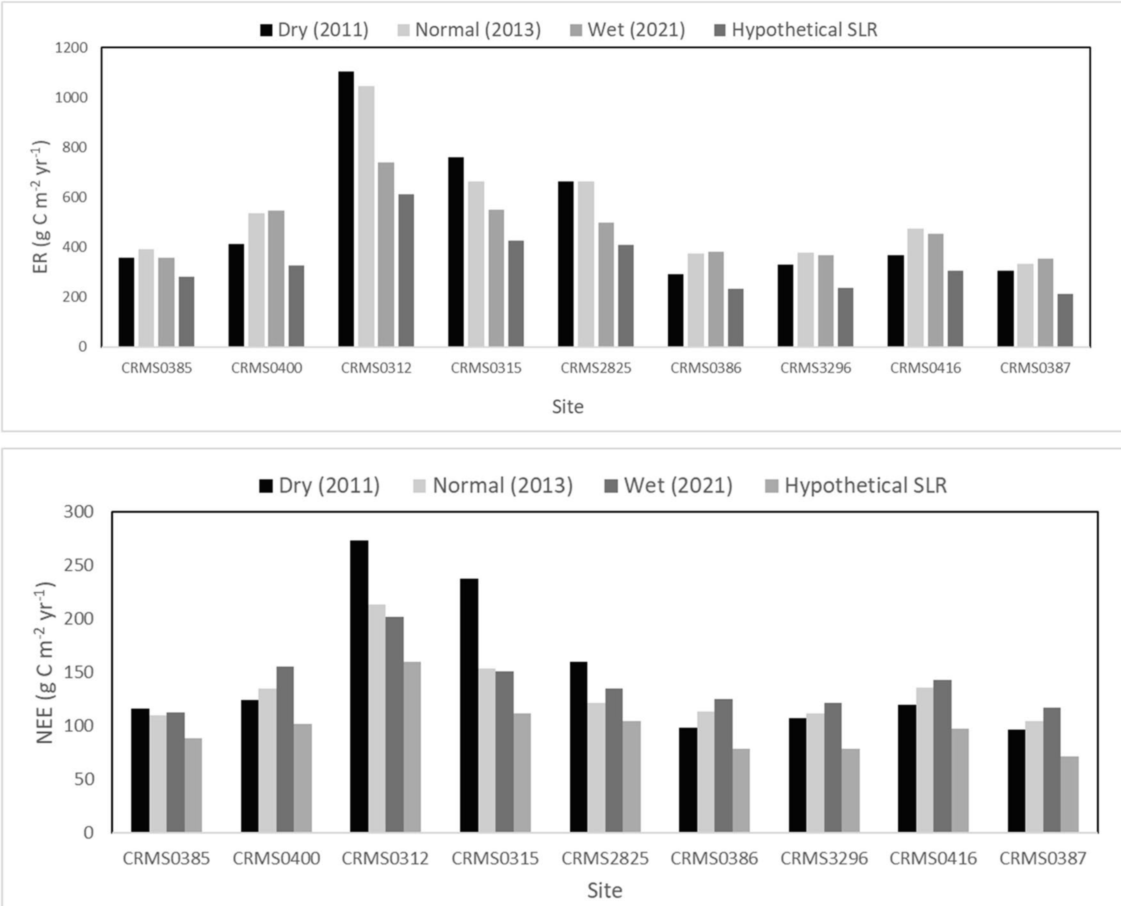

Fig. 5 Simulated ER and NEE under the dry, normal, wet, and hypothetical SLR conditions in the brackish marsh sites in Terrebonne Basin, Louisiana

Impacts of Marsh Inundation, Drought, and Hypothetical SLR

The two-way ANOVA also showed that there were significant "scenario" and "site × scenario" effects ($p < 0.0001$) for NEE, GPP, ER, CH_4 and N_2O fluxes (Table S1), indicating that marsh inundation, drought, and SLR significantly affected NEE, GPP, ER, CH_4 and N_2O fluxes and the responses of these fluxes to climate change scenarios varied significantly among the tidal brackish marsh sites. One-way ANOVAs (Table S2) for each of the nine brackish marsh sites determined the sites with significant ($p < 0.05$) impacts of drought, inundation, and hypothetical SLR conditions on NEE, GPP, ER, CH_4 and N_2O fluxes.

Compared to the normal year, GPP decreased significantly ($p < 0.0001$, Table S2) at six sites by average −17% in the dry year, at five sites by average −20% in the wet year, and all nine sites by average −40% in the hypothetical SLR case (Fig. 4). ER decreased significantly ($p < 0.0001$, Table S2) at five sites by average −20% in the dry year, at four sites by average −22% in the wet year, and all nine sites by average −37% in the hypothetical SLR case (Fig. 5). Only one exception is CRMS0315 which had increased ER in the dry year compared to the normal year, a 15% increase (Fig. 5). The response of NEE to the climate change scenarios differed from that of GPP and ER. Under the dry year condition, NEE increased (or release more CO_2 to the atmosphere) significantly ($p < 0.0001$, Table S2) at CRMS0312, CRMS0315, and CRMS2825 whereas NEE decreased significantly ($p < 0.0001$, Table S2) at CRMS0386 and CRMS0416, compared to the normal year (Fig. 5). Under the wet year condition, NEE increased significantly ($p < 0.0001$, Table S2) at CRMS0400, CRMS0386, and CRMS0387 compared to the normal year (Fig. 5). In contrast, NEE decreased significantly ($p < 0.0001$, Table S2) at all sites except CRMS0312 and CRMS2825 under the hypothetical SLR condition compared to the normal year (Fig. 5). The different spatial patterns of GPP, ER, and NEE under different hydrologic conditions (wet, dry, SLR) can be explained by variability in marsh surface elevation at these brackish marsh sites that determined the various changes in soil salinity and water table depth under different hydrological conditions

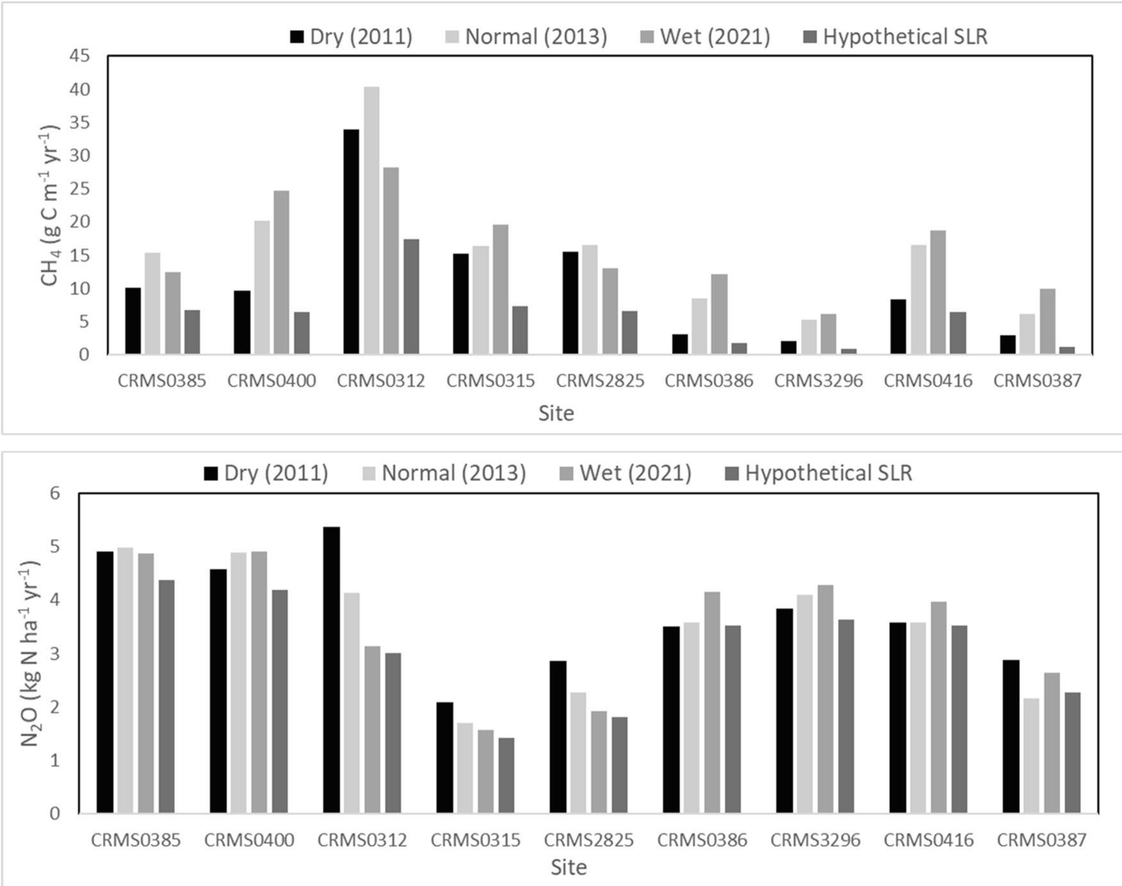

Fig. 6 Simulated CH_4 and N_2O emissions under the dry, normal, wet, hypothetical SLR conditions in the brackish marsh sites in Terrebonne Basin, Louisiana

across sites. For example, the increase rather than decrease in GPP at CRMS0315 under the dry year compared to the normal year could be largely attributed to the least increase in soil salinity (< 1.7 psu) among all the brackish marsh sites (1.8–5.4 psu) (Table 2). The increase (+ 4.3%) rather than decrease in GPP at CRMS0387 under the wet year compared to the normal year can be explained by the reduced stress from both inundation (from 69.4 cm to 51.5 cm) and soil salinity (from 11.6 psu to 9.6 psu) compared to other sites with increased inundation and slightly decreased soil salinity (Table 2).

Compared to the normal year, CH_4 emissions decreased significantly ($p < 0.0001$, Table S2) at six sites in the dry year and at all sites in the hypothetical SLR condition (Fig. 6). In the wet year, CH_4 emissions decreased significantly at CRMS0385, CRMS0312 and CRMS2825, but increased significantly at CRMS0400, CRMS0386 and CRMS0387 ($p < 0.0001$, Table S2), compared to the normal year (Fig. 6). Mean CH_4 emissions across the nine sites decreased by −38% and −67% in the dry year and hypothetical SLR condition whereas cross-site CH_4 emissions increased by 12% in the wet year. N_2O emissions also increased significantly at CRMS0312, CRMS0315, CRMS2825, and CRMS0387 whereas decrease significantly at CRMS0400 and CRMS3296 ($p < 0.0001$, Table S2) in the dry year compared to the normal year (Fig. 6). In the wet year, N_2O emissions increased significantly at CRMS0315, CRMS0386, CRMS0416, and CRMS0387 whereas N_2O emissions decreased significantly at CRMS0312 and CRMS2825 ($p < 0.0001$), compared to the normal year (Fig. 6). N_2O emissions decreased significantly ($p < 0.0001$) at most sites excluding CRMS0386 and CRMS0416 and increased significantly at one site (CRMS0387) (Fig. 6).

WCAT-DNDC also predicted NPP, plant and soil respiration (plant CO_2 and soil CO_2) under the different climate scenarios. NPP decreased under the dry, wet years and hypothetical SLR condition compared to the normal year at all sites (except CRMS0387 in the dry year), ranging from −13% to −100% (Table 3). Under the drought condition, plant respiration decreased at all sites except CRMS0312 and CRMS0315, ranging from −5% to −27% with site averaged decrease of −18% (Table 3). In the wet year, NPP also

Table 3 Simulated NPP, plant and soil respiration and change percentage under the normal, dry, wet, and hypothetical SLR conditions in the brackish marsh sites in Terrebonne Basin, Louisiana

Site	Normal (2013)	Dry (2011)	Wet (2021)	Hypothetical SLR	Change (%): Dry to Normal	Change (%): Wet to Normal	Change (%): Hypothetical SLR to Normal
NPP (g C m^{-2} yr^{-1})							
CRMS0385	14.97	3.13	7.57	6.04	-79.09	-49.40	-59.66
CRMS0400	27.64	10.45	15.28	3.51	-62.20	-44.72	-87.32
CRMS0312	83.66	56.00	13.63	15.80	-33.06	-83.71	-81.11
CRMS0315	57.94	29.61	22.98	21.68	-48.89	-60.35	-62.59
CRMS2825	79.62	68.96	14.86	16.69	-13.38	-81.33	-79.03
CRMS0386	3.91	1.90	2.22	1.56	-51.39	-43.29	-60.03
CRMS3296	11.37	9.34	3.23	4.32	-17.91	-71.62	-62.05
CRMS0416	9.26	1.61	3.51	2.69	-82.65	-62.03	-70.93
CRMS0387	0.49	6.97	0.00	0.15	1336.80	-100.00	-68.75
Plant CO_2 (g C m^{-2} yr^{-1})							
CRMS0385	354.81	315.18	311.71	248.15	-11.17	-12.15	-30.06
CRMS0400	497.07	364.62	500.38	291.10	-26.65	0.67	-41.44
CRMS0312	997.93	1024.65	691.75	574.54	2.68	-30.68	-42.43
CRMS0315	602.92	652.59	498.28	385.43	8.24	-17.35	-36.07
CRMS2825	611.55	578.32	462.28	378.68	-5.43	-24.41	-38.08
CRMS0386	339.67	251.86	339.91	202.29	-25.85	0.07	-40.45
CRMS3296	340.36	278.41	321.94	204.66	-18.20	-5.41	-39.87
CRMS0416	436.46	326.03	409.72	273.14	-25.30	-6.13	-37.42
CRMS0387	302.04	265.15	315.43	184.42	-12.21	4.43	-38.94
Soil CO_2 (g C m^{-2} yr^{-1})							
CRMS0385	37.14	42.97	43.98	34.26	15.68	18.41	-7.77
CRMS0400	38.59	46.90	46.35	34.47	21.51	20.08	-10.68
CRMS0312	47.92	79.66	46.29	36.61	66.25	-3.39	-23.59
CRMS0315	60.48	106.81	51.08	40.27	76.60	-15.55	-33.42
CRMS2825	50.91	85.68	36.62	29.28	68.30	-28.06	-42.49
CRMS0386	33.02	40.21	42.32	31.63	21.78	28.18	-4.21
CRMS3296	37.72	50.01	44.21	33.35	32.59	17.21	-11.59
CRMS0416	36.52	42.28	44.77	33.67	15.76	22.58	-7.81
CRMS0387	29.69	41.02	38.71	27.89	38.16	30.38	-6.06

decreased at most sites except CMRS0400, CRMS0386 and CRMS0387 where a slight increase in NPP occurred (Table 3). Plant respiration was inhibited at all sites under the hypothetical SLR condition, ranging from −30% to −43% (Table 3). Soil respiration rates were enhanced by 16 – 77% in the dry year compared to the normal year. In contrast, soil respiration was inhibited at all sites by −4 to −43% under the hypothetical SLR condition compared to the normal year (Table 3). In the wet year, both increased (17–31%) and decreased (−3 to −28%) soil respiration rates occurred, compared to the normal year (Table 3).

The results of the numerical experiment for thresholds of soil salinity and water table depth on NEE showed that for the degrading brackish marshes in Terrebonne Basin, very high salinity and water levels can significantly reduce NEE but the minimum NEE is around 30 g C m^{-2} yr^{-1} (Fig. 7). In other words, unrealistic salinity and water levels could minimize C loss from these wetlands but no combination of the two would lead to C sequestration.

Discussion

Spatial Variability in Carbon and GHG Fluxes

Our first key finding is that there are large spatial variations in carbon and GHG fluxes in tidal brackish marshes even with same or similar dominant plant species composition and distribution and similar hydrogeomorphic setting within the Terrebonne Bay, Louisiana, USA. Large variability in marsh surface elevation, incoming tidal surface water salinity, and surface water level, together determine the variable

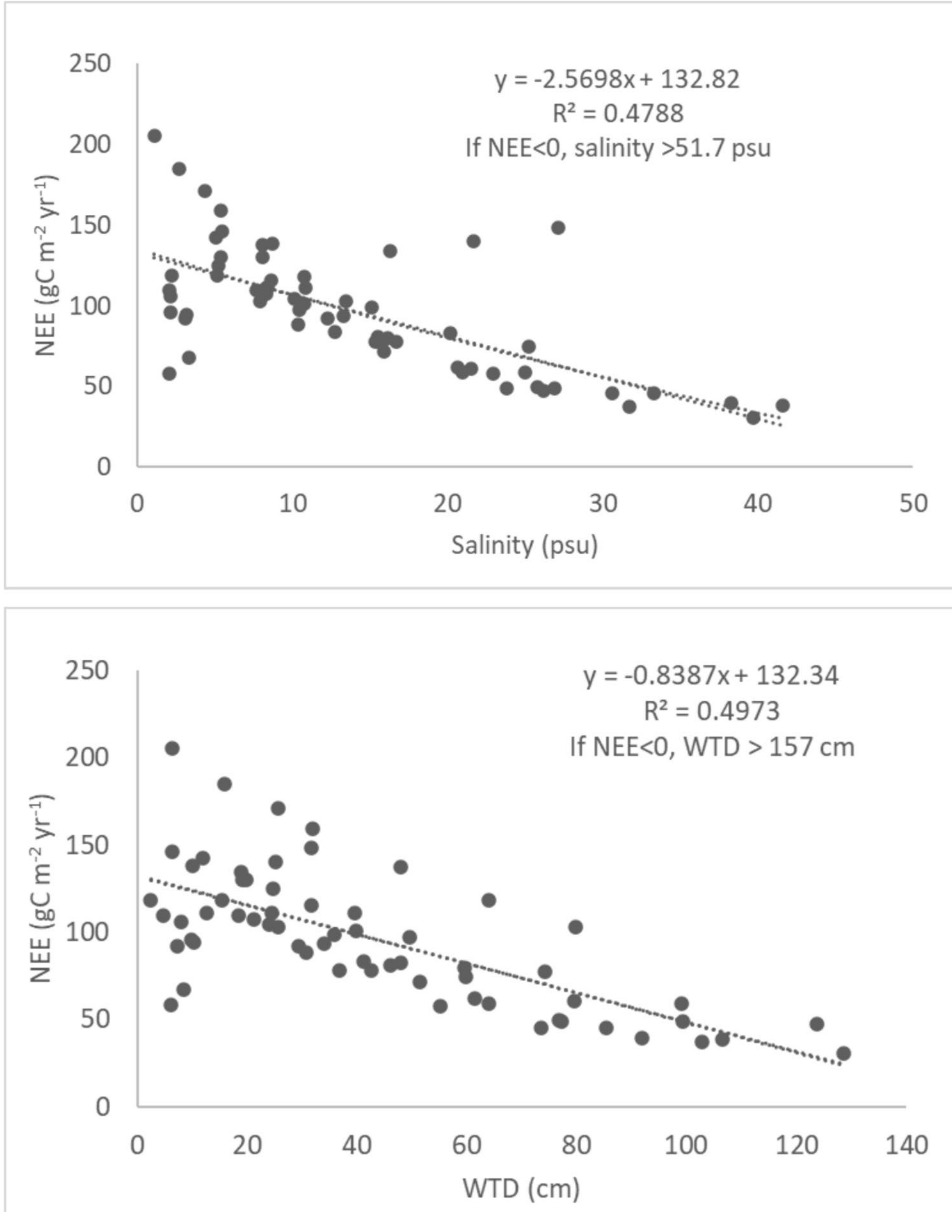

Fig. 7 Relationships between simulated NEE and soil salinity and water table depth (WTD) conditions in the brackish marsh sites in Terrebonne Basin, Louisiana

soil porewater salinity and soil water depth (moisture level) regime of a wetland location, which in addition to the large variability in soil organic matter (carbon) content, are attributed to the spatial variability in NEE, GPP, ER, CH_4 and N_2O fluxes across these brackish marshes. Considering the normal, wet and dry years together, the ranges of carbon and GHG fluxes were 96.3 to 273.3, 194 to 832.6, 292.1 to 1104.3, and 2.1 to 40.4 g C m^{-2} yr^{-1} for NEE, GPP, ER, CH_4 and 1.7 to 5.4 kg N ha^{-1} yr^{-1} for N_2O, respectively. Here, the positive values for NEE, CH_4 and N_2O indicate net emission (sources) of CO_2, CH_4 and N_2O to the atmosphere. Tidal brackish marshes have been found to emit as much as 1011 g C m^{-2} yr^{-1} to the atmosphere when marshes are in degradation and uptake as high as −804 g C m^{-2} yr^{-1} when they are healthy or restored from degradation (Knox et al. 2014; Krauss et al. 2016; Wilson et al. 2015, 2018a, b; Ishtiaq et al. 2022). At CRMS2825, Krauss et al. (2016) used the static chamber method to measure the NEE and found a much higher rate of NEE occurred (1011 g C m^{-2} yr^{-1}) at this site compared to the 170.6 g C m^{-2} yr^{-1} measured by the EC method. Although static chambers capture small/local scale variations in CO_2 and may result in higher uncertainty in scaled NEE than the EC method over a larger area and longer period (Krauss et al. 2016), the higher NEE indicated the high potential of CO_2 release from the degrading brackish marshes. In a brackish marsh site in Bayou Dularge in Terrebonne Bay, Louisiana, it was found that the brackish marsh emitted 447 g C m^{-2} yr^{-1} in a reference location compared to 164 g C m^{-2} yr^{-1} in a location with herbicide treatment (Lane et al. 2016), suggesting that brackish marshes in Terrebonne Basin are acting as carbon sources to the atmosphere even under normal or reference conditions without further natural and anthropogenic disturbances. Net emissions of CO_2 were also observed from other degrading tidal brackish marshes along the Gulf coast (Wilson et al. 2015, 2018a, b, Ishtiaq et al. 2022). Wilson et al. (2018a, 2018b) found that soil water level dry-down and increased salinity at Everglades brackish marsh sites released 32 to 454 g C m^{-2} yr^{-1}. There are no data on NEE in Terrebonne brackish marshes when they were healthy with connection with riverine sediment, but data from healthy and restored tidal brackish marshes in other coastal areas showed that as high as −804 g C m^{-2} yr^{-1} of net uptake of CO_2 could occur from restored brackish marshes (Knox et al. 2014). Large spatial variability in NEE across the brackish marshes in this study can be explained by the variations in GPP and ER in the study area since NEE is determined by GPP and ER.

GPP also varied greatly across the selected nine brackish marsh sites in Terrebonne Basin, Louisiana, ranging from 194 to 833 g C m^{-2} yr^{-1}. Limited studies showed that a large range of 174 to 1628 g C m^{-2} yr^{-1} existed for tidal brackish marshes and less than 550 g C m^{-2} yr^{-1} occurred for degrading brackish marshes (Holm et al. 2016; Krauss et al. 2016; Lane et al. 2016; Wilson et al. 2018a, b; Chamberlain et al. 2019). For instance, dry-down events with increased soil salinity (about 20 psu) at the brackish marsh in Everglades National Park, Florida resulted in low GPP from 440 to 520 g C m^{-2} yr^{-1} (Wilson et al. 2018a) and from 174 to 285 g C m^{-2} yr^{-1} relative to control treatment at a site in Shark River Slough, Florida (Wilson et al. 2018b). In relatively healthy brackish marshes along the Atlantic and Gulf coasts, GPP was found to be in the range of 650–1000 g C m^{-2} yr^{-1} (Krauss et al. 2016). In this study, all the brackish marsh sites except CRMS0312 had GPP less than 550 g C m^{-2} yr^{-1}, indicating that these brackish marshes are under stress from climate-induced changes in salinity and water level regimes that reduce plant growth (Janousek and Mayo 2013; Snedden et al. 2015; Janousek et al. 2020). Large GPP at CRMS0312, the floating marsh, is likely due to the high soil organic matter content (Table 1) providing more nutrient for plant growth and the reduced stress on plant growth from prolonged flooding or drought and drought-induced salinity intrusion (Table 2) by its capability to rise and fall with water levels. It was found that *S. patens* productivity was significantly higher in treatment with high organic content and nutrient enrichment than that with high bulk density but low organic content from sediment addition (Matzke and Elsey-Quirk 2018).

There were large variations in ER across the tidal brackish marshes, averaging approximately 507 g C m^{-2} yr^{-1} with a range of 292 to 1104 g C m^{-2} yr^{-1} under the normal, wet and dry years. Previous tidal brackish marsh studies found that ER varied between 228 to 1496 g C m^{-2} yr^{-1} (Nyman and DeLaune 1991; Krauss et al. 2016; Wilson et al. 2015, 2018a, b). Lower ER rates were found at brackish marsh sites in Barataria Basin, Louisiana (228 g C m^{-2} yr^{-1}, Nyman and DeLaune 1991) and in Mobile Bay, Alabama (281 g C m^{-2} yr^{-1}, Wilson et al. 2015). Higher ER rates (389 to 948 g C m^{-2} yr^{-1}) were found at brackish marshes in Everglades during droughts (Wilson et al. 2018b). These data showed that the selected brackish marsh sites in Terrebonne Basin, Louisiana, responded to drought with slightly decreased plant (stem and root) respiration but large increases in soil heterotrophic respiration (Table 3). Large spatial variability in ER across the brackish marsh sites could be attributed to the variation of soil properties. High organic matter content at floating marsh CRMS0312 could provide a rich substrate for microbes, leading to higher rates of organic decomposition and respiration from the greater microbial activity in the organic-rich environment. In contrast, at attached marshes such as CRMS0315 and CRMS3296 with higher bulk density (> 0.23 g cm^{-3}, Table 1) can limit oxygen diffusion, hinder microbial activity, leading to lower ER rates (Luo et al. 2019).

The tidal brackish marshes were net sources of CH_4 and N_2O emission under the normal, wet, and dry years. While a large range of methane emission (2.5 to 404) was found for tidal marshes including freshwater marshes (Poffenbarger et al. 2011), previous studies found that tidal brackish marshes tended to have net CH_4 emission in the range of −0.16 (uptake) to 73 g C m^{-2} yr^{-1} (Nyman and DeLaune 1991; Holm et al. 2016; Krauss et al. 2016; Lane et al. 2016; Chamberlain et al. 2019). CH_4 emission would not exceed 70 g C m^{-2} yr^{-1} even under degradation (Lane et al. 2016). For instance, tidal brackish marshes emitted 9.5 g C m^{-2} yr^{-1} of CH_4 when treated with herbicide compared to 7.0 g C m^{-2} yr^{-1} at the reference site (Lane et al. 2016). CH_4 emissions were −0.3 g C m^{-2} yr^{-1} (uptake) to 2.31 g C m^{-2} yr^{-1} at brackish marshes exposed to sea level rise and saltwater intrusion (Ishtiaq et al. 2022). There were very few studies on N_2O emissions from tidal brackish marshes. N_2O emission at CRMS2825 was 1.2 kg N ha^{-1} yr^{-1} in another study (Krauss et al. 2016). N_2O emissions were low under both herbicide treatment (0.16 4 kg N ha^{-1} yr^{-1}) and reference (0.17 4 kg N ha^{-1} yr^{-1}) sites in Terrebonne Basin, Louisiana (Lane et al. 2016). The large range of N_2O emission found in this study indicated a large spatial variation in N_2O fluxes in the degrading tidal brackish marshes in MRDP. Spatial variability in CH_4 and N_2O fluxes across the brackish marshes in this study could be attributed to the synergic effect of soil salinity and water table depth, which showed large variation across the sites (Table 2). It was found that CH_4 and N_2O fluxes decreased with increasing salinity and inundation larger than 10 cm above marsh surface due to the inhibition of methanogenesis, nitrification ad denitrification (Wang et al. 2023a, b).

Impacts of Climate Scenarios

Our second key finding is that both drought and inundation will exacerbate carbon loss from the brackish marshes experiencing a transition from an initially healthy to deteriorated stage in an inactive basin of MRDP due to marsh disconnecting with freshwater and sediment delivery (Cassaway et al. 2024). The studied tidal brackish marshes emitted CO_2 to the atmosphere at an average rate of 132 g C m^{-2} yr^{-1} (range: 104 – 213) in the normal year and this rate increased to 140 g C m^{-2} yr^{-1} (range: 112 – 202 g C m^{-2} yr^{-1}) in the wet year, and to 148 g C m^{-2} yr^{-1} (range: 96 – 273) in the dry year (Fig. 8). Tidal brackish marshes at other coastal areas such as Florida Everglade and Alabama Mobile Bay were also found to be net CO_2 emissions and blue carbon loss increased under harsh environments (e.g., elevated surface water and soil porewater salinity and dry-down of soil water due to saltwater intrusion) (Wilson et al. 2015; Wilson et al. 2018a, b; Ishtiaq et al. 2022). Wilson et al. (2015) found that a brackish marsh along the Mobile Bay, Alabama, was a net CO_2 emitter with seasonal exposure to saltwater intrusion that depressed plant productivity and increase organic matter remineralization, leading to greater blue carbon loss. The brackish marsh was in a state of transition from oligohaline (0.5 – 5 psu) to mesohaline (5 – 15 psu) marshes (Wilson et al. 2015).

In this study, the increase in net CO_2 emissions is driven by the large reduction in NPP and the increased soil respiration compared to the normal year (Table 3) under the stress of elevated soil salinity and drought or inundation. Carbon losses from tidal brackish marshes were also found in other coastal areas and declines in plant productivity was recognized as the major driving factor (Wilson et al. 2018a, b; Ishtiaq et al. 2022). Within brackish marshes in Everglades National Park, Florida, elevated salinity interacted with hydroperiod to determine gross and net ecosystem productivity and ecosystem respiration (Wilson et al. 2018a). During exposed periods with elevated salinity, CO_2 efflux increased three times (334 to 454 g C m^{-2} yr^{-1}) at the Everglades brackish marshes due to large decrease (72%) in live root biomass that led to observed peat soil collapse (Wilson et al. 2018a, b). With the increase in soil salinity, the growth of marsh plant or carbon fixation of the dominant species (i.e., *S. patens*) is largely inhibited (Snedden et al. 2015; Krauss et al. 2016). Additionally, shifts in salinity levels and flood duration due to natural processes or human activities can lead to changes in vegetation composition and

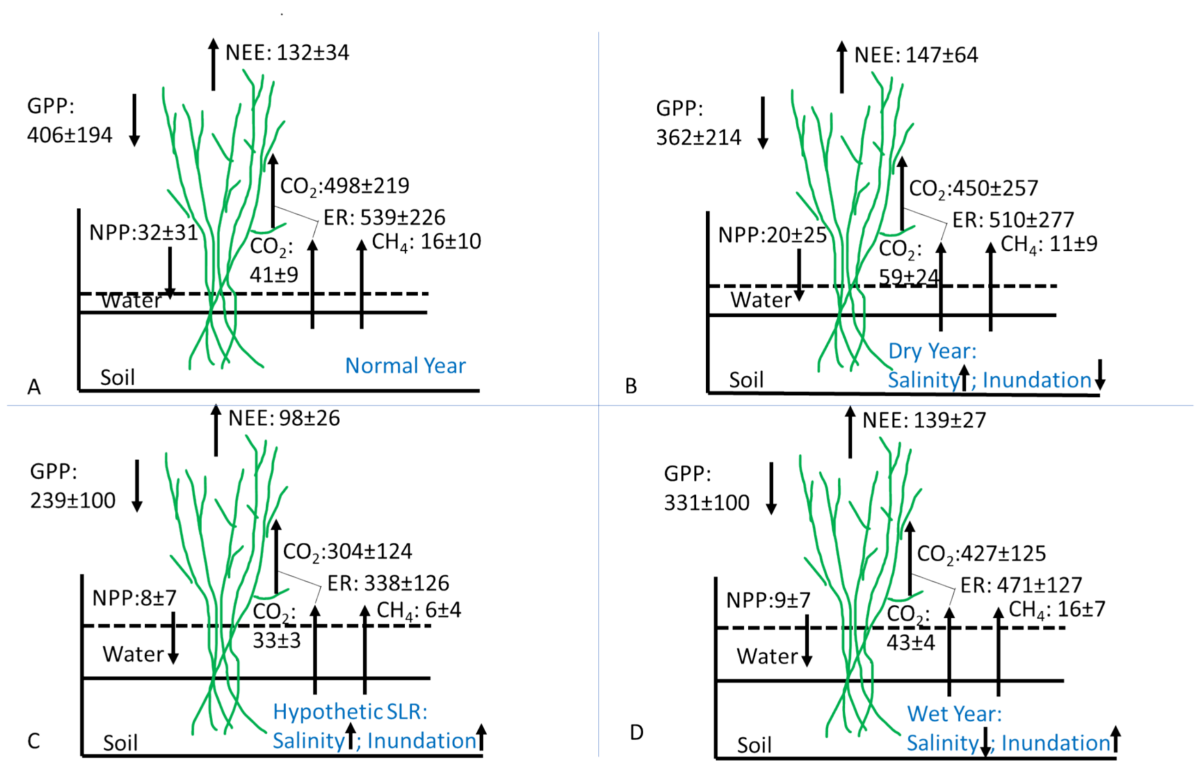

Fig. 8 Diagram showing the averaged carbon fluxes (unit: g C m^{-2} yr^{-1}) under the normal, dry, wet years, and hypothetical SLR in the brackish marsh sites in Terrebonne Basin, Louisiana using WCAT-DNDC. Note: Arrows are not scaled by the fluxes, arrow directions indicate input or output of the fluxes, soil depth in the model is 50 cm

marsh types with different plant productivity. For instance, increased salinity might favor the growth of *S. alterniflora*, a dominant species for salt marshes that is also well-adapted to flooding. Average annual salinity for brackish and salt marshes are approximately 10 psu and 16 psu (Snedden 2018). Since the average annual salinity at the brackish sites except CRMS0312 in the dry year were larger than 10 psu (Table 2), it is likely that these brackish marshes will change to salt marshes under continued drought conditions. In fact, marsh types at these sites have changed since establishment in 2006 among intermediate, brackish and salt marshes due to the changes in dominant species associated with changes in salinity and inundation regimes. For example, CRMS2825 were classified as intermediate marsh in 2014, 2015, and 2016, backed to brackish marsh in 2017 until 2022, but shifted to salt marsh in 2023 (CRMS, https://www.lacoast.gov/crms/Home.aspx) due to drought events in 2023. It was found that above- and belowground biomass was lower in *S. alterniflora* than in *S. patens* when inundation was minimal (Snedden et al. 2015). Biomass in the two species decreased exponentially with increased flood duration and this negative biomass response to flooding tended to be more pronounced in *S. patens* than in *S. alterniflora* (Snedden et al. 2015). High salinity induced declining GPP could be attributed to decreased plant photosynthesis, photosynthetic pigment concentrations, and stomatal conductance (Luo et al. 2019; Li et al. 2020). With higher salinity, metabolic products such as sulfide will increase, stressing marsh plants and decreasing productivity as well as leading to toxic effects on marsh roots (e.g., Wilson et al. 2015).

Reduced ER with increased salinity could be attributed to the suppressed growth of plants and soil microorganisms (Weston et al. 2014; Krauss et al. 2016; Li et al. 2020). Analysis of simulation results of a biogeochemistry model with similar structure as WCAT-DNDC indicated that when soil water table declines during drought and changes from saturated to unsaturated conditions, oxidative reactions including methanotrophy, nitrification, and decomposition are enhanced, leading to the increase in soil CO_2 emission and decrease in CH_4 emission in low salinity tidal wetlands including marshes (Wang et al. 2023a). Inundation was found to reduce oxygen level (low redo potential), reduce leaf gas exchange and light availability, and build up toxic hydrogen sulfide in plant tissue (e.g., Janousek et al. 2020; Li et al. 2020). Both the Everglades coastal brackish marsh study (Wilson et al. 2018a, b) and our Terrebonne brackish marsh study confirm that declines in marsh plant productivity from elevated salinity and marsh exposure to drought and/or inundation play a critical role in increased blue carbon loss, consequently, the collapse of marsh soils, and eventually export of carbon out of the ecosystem by erosive forces (wind, waves, and current). Under the hypothetical SLR condition, net emission of CO_2, GPP, NPP, plant and soil respiration were reduced compared to the normal year (Figs. 4, 5, 8, Table 3). This could be due to high salinity exacerbating the effects of increasing inundation on plant productivity, or dual, severe suppression of growth (Janousek and Mayo 2013; Janousek et al. 2020; Li et al. 2020). In a long-term (33 years) field study of tidal brackish marsh on the Chesapeake Bay, USA, Zhu et al. (2022) found that plant productivity especially root production declined when sea level was above the 15-cm NAVD88 threshold due to the increase in inundation resulting in the diminished elevated CO_2 stimulation of production.

In this study, the tidal brackish marshes in the Terrebonne Basin were found to be net sources of CH_4 and N_2O under the climate scenarios. Large CH_4 effluxes (~ 17 g C m^{-2} yr^{-1}) were also found at other tidal brackish marshes such as the oligohaline marsh site along the Delaware River Estuary (e.g., Weston et al. 2014). Nevertheless, CH_4 emissions decreased in all nine sites under the dry year and decreased even more under the hypothetical SLR case in this study. Other tidal marsh sites along the Gulf coast, such as a degraded brackish marsh in Mobile Bay, showed lower CH_4 efflux compared to our study (e.g., Wilson et al. 2015). Such decreases in CH_4 emissions could be attributed to the inhibition of methanogenesis due to the increased activities of sulfate-reducing bacteria with increased soil salinity and the increased CH_4 oxidation by methanotrophic bacteria at the soil-atmosphere interface zone and the rhizospheric zone (Wilson et al. 2015; Wang et al. 2023a).

For N_2O emissions, the fluxes were found to increase or decrease in dry and wet years and decrease at most of the sites under the hypothetical SLR case. The complicated N_2O change pattern reflected the synergic effect of soil water table depth and soil salinity and indicate that soil water table depth plays a more important role than soil salinity. The finding on N_2O emissions in this study are consistent with previous studies on low salinity marshes (< 10 psu), which found that N_2O emissions were largely controlled by soil water level rather than soil salinity and N_2O emissions declined greatly with rising water level when soils were not inundated, and emissions were low when soils were inundated (Wang et al. 2023a, b). The increase in N_2O fluxes in some of the tidal brackish marshes (CRMS0312, CRMS0315, CRMS2825) in this study under drought condition could largely be attributed to the stimulation of nitrification that produce N_2O during NH_4^+ oxidation under drought condition (Wang et al. 2023a). In contrast, other brackish marsh sites were mostly inundated under normal, dry, and wet years, forming anaerobic conditions, resulting in more N2O emission from denitrification (Luo et al. 2019; Wang et al. 2023a). Furthermore, it was found that the hypothetic SLR, dry, and wet year induced average changes were approximately −67%, −38% and + 12% for CH_4 emission, and −13%, + 11% and + 0.5% for N_2O emission, suggesting that the hypothetic SLR played a more pronounced effect on GHG fluxes than dry and wet condition, dry condition played a more pronounced effect on GHG fluxes than the wet condition.

Implications for Coastal Wetland Restoration

The climate scenario results illustrate that carbon loss in degrading tidal brackish marshes in inactive basins of MRDP will be amplified under drought and inundation conditions. The exacerbated carbon loss poses a big challenge to tidal wetland persistence, especially brackish marsh restoration, under future climate change. Without tidal wetland restoration actions, the previously stored blue carbon in vegetation and soil pools will eventually disappear, released to the atmosphere as gas or with water to estuaries via peat collapse and conversion to open water (Wilson et al. 2015; Lane et al. 2016; Wang et al. 2017; Wilson et al. 2018a, b; Baustian et al. 2021; Ishtiaq et al. 2022). The State of Louisiana's Coastal Master Plan modeling results estimated that coastal Louisiana marshes can be expected to decrease their total long-term carbon burial after 50 years from 4.3 Tg C yr^{-1} in 2013 to 2.1 Tg C yr^{-1} with no coastal restoration, a reduction of about 50% (Baustian et al. 2021). Wetland morphology modeling results indicated that large river diversions could improve basin-wide soil organic carbon sequestration capacity (162–222 g C m^{-2} yr^{-1}) by up to 14% (30 g C m^{-2} yr^{-1}) in Louisiana deltaic wet-lands compared to the future-without-action scenario (Wang et al. 2017). The turning back to being a net CO_2 sink from a net CO_2 source for these tidal brackish marshes depends on the healthy and enhanced marsh productivity to sequester and store sufficient blue carbon by successful tidal wetland restoration. Marsh creation to establish new wetlands in open water areas using dredged material and sediment diversions to existing marshes are two critical techniques for tidal wetland restoration in coastal Louisiana (CPRA 2017). Sediment diversions also help lower salinity and stimulate growth of brackish marshes in addition to increasing sediment deposition on marsh surface (e.g., DeLaune et al. 2005).

Results from this type of simulation study can inform operational restoration project. For example, the Terrebonne Basin Ridge and Marsh Creation Project (CPRA 2017) includes blue carbon credit/offset to mitigate climate change in project success assessment. Meanwhile, since tidal brackish marshes are susceptible to elevated salinity and hydrologic alterations, hydrologic restoration (e.g., freshwater diversions) and salinity control structures (e.g., local flap-gated culverts) may be necessary with marsh creation projects to prevent carbon loss and restore the net carbon sink capacity of these tidal brackish marshes. For example, it was found that simulated daily NEE, GPP and ER fluxes in the summer at CRMS0400 in the wet year showed little difference with that in the normal year even though inundation depth could be 10–30 cm larger in the wet year than that in the normal year during the summer period. Increased NEE and reduced GPP with increased water table depth (inundation depth), thus increased net emission of CO_2 to atmosphere, occurred mostly in late spring (February to April). Therefore, carbon flux changes from this study could also be considered in the operation (timing and discharge) of freshwater diversion (e.g., the increase Atchafalaya Flow to Terrebonne Diversion, CPRA 2017) not only for controlling (reducing) salinity but also for maintaining ecosystem functions such as carbon sequestration. The threshold numerical experiment showed that although very high salinity and water levels can significantly reduce NEE but minimum NEE is still positive (approximately 30 g C m^{-2} yr^{-1}, suggesting that controlling soil salinity and water table depth only could not turn the marshes into net uptake of CO_2. These results indicated that healthy marsh and enhanced primary productivity via increasing sediment/nutrient inputs (e.g., DeLaune et al. 2005) should be the primary restoration approach for restoring marsh net uptake of CO_2 or carbon sink.

Conclusions

A wetland biogeochemistry model, WCAT-DNDC was validated and applied to nine tidal brackish marshes in Terrebonne Basin, Louisiana, a coastal basin with minimal freshwater and sediment inputs and high rates of relative SLR. Using this model, carbon and GHG fluxes including NEE, GPP, ER, CH_4 and N_2O were evaluated in simulation scenarios of a normal climate and under inundation, drought and hypothetical SLR conditions with changes in both soil salinity and water level regimes. It was found that all these tidal brackish marshes were net CO_2 emitters to the atmosphere under the normal year and blue carbon loss will increase under both drought and inundation conditions. The increase in net CO_2 emissions is mainly driven by the large reduction in primary productivity and the increased ecosystem respiration especially soil respiration under drought and inundation conditions. Net CO_2 emissions were reduced under the hypothetical SLR scenario with increases in both soil salinity and inundation duration, reflecting the synergic effect of salinity and inundation (substantial reduction) on plant productivity and ecosystem respiration. Without tidal wetland restoration actions, the previously stored blue carbon in vegetation and soil pools will eventually be gone to the atmosphere and with water to estuaries via peat collapse and conversion to open water. The model and simulation results of different climate change scenarios can be helpful for the assessment of carbon budget, carbon credit and climate mitigation offset potential of tidal wetland restoration projects such as the ongoing marsh creation, hydrologic restoration, and salinity control projects as well as informing the design and implement of future projects in MRDP.

Supplementary Information The online version contains supplementary material available at https://doi.org/10.1007/s13157-024-01881-w.

Acknowledgements This research was supported by funds from the U.S. Geological Survey (USGS) Climate Research and Development Program, the USGS Ecosystems Mission Area, and the NASA Carbon Monitoring Systems program to the U.S. Department of Agriculture Forest Service. We thank the Coastwide Reference Monitoring System (CRMS) of the U.S. Congress enacted the Coastal Wetlands Planning, Protection, and Restoration Act (CWPPRA) for providing hydrology, soil, and vegetation at the brackish marshes and the FLUXNET Network for providing daily GPP, ER, NEE and CH_4 at CRMS2825. Climate data were provided by the Oak Ridge National Laboratory's Daily Surface Weather and Climatological Summaries (Daymet) database. We thank Kevin J. Buffington and two anonymous reviewers for their constructive review for improving this manuscript. Any use of trade, firm, or product names is for descriptive purposes only and does not imply endorsement by the U.S. Government.

Author Contributions H.W: Study design, field data collection, data analysis, modeling, and manuscript writing.

K.K: Field data collection, data analysis, manuscript writing.

Z.D: Modeling, data analysis, and manuscript writing.

G.N: Field data collection, data analysis, manuscript writing.

C.T: Modeling, data analysis, and manuscript writing.

Funding This work was supported by the U.S. Geological Survey (USGS) Climate Research and Development Program, the USGS Ecosystems Mission Area, and the NASA Carbon Monitoring Systems program to the U.S. Department of Agriculture Forest Service.

Data Availability The datasets generated during the current study are available from the corresponding author on reasonable request.

Declarations

Competing Interests The authors have no relevant financial or non-financial interests to disclose.

References

Adame MF, Kelleway J, Krauss KW, Lovelock CE, Adams JB, Trevathan-Tackett SM et al (2024) All tidal wetlands are blue carbon ecosystems. BioScience 74:253–268

Bansal S, Creed IF, Tangen BA, Bridgham SD, Desai AR, Krauss KW et al (2023) Practical guide to measuring wetland carbon pools and fluxes. Wetlands 43(8):105

Baustian MM, Stagg CL, Perry CL, Moss LC, Carruthers TJB (2021) Long-term carbon sinks in marsh soils of coastal Louisianan are at risk to wetland loss. Journal of Geophysical Research: Biogeosciences 126:e2020JG005832. https://doi.org/10.1029/2020JG005832

Bridgham SD, Megonigal JP, Keller JK, Bliss NB, Trettin C (2006) The carbon balance of Norther American wetlands. Wetlands 26:889–916

Cassaway AF, Twilley RT, Rovai AS, Snedden GA (2024) Patterns of marsh surface accretion rates along salinity and hydroperiod gradients between active and inactive coastal deltaic floodplain. Estuarine, Coastal and Shelf Science 301:108757

Chamberlain SD, Hemes KS, Eichelmann E, Szutu DJ, Verfaillie JG, Baldocchi DD (2019) Effect of drought-induced salinization on wetland methane emissions, gross ecosystem productivity, and their interactions. Ecosystems 23:675–688

Coastal Protection and Restoration Authority (CPRA) of Louisiana (2024) Coastwide Reference Monitoring System-Wetlands Monitoring Data. Retrieved from Coastal Information Management System (CIMS) database. http://cims.coastal.louisiana.gov. Accessed 23 Mar 2024

Dai Z, Trettin CC, Li C, Li H, Sun G, Amatya DM (2012) Effect of assessment scale on spatial and temporal variations in CH_4, CO_2 and N_2O fluxes in a forested watershed. Water, Air, and Soil Pollution 223:253–265

Dai Z, Trettin CC, Frolking S, Birdsey RA (2018) Mangrove carbon assessment tool: Model development and sensitivity analysis. Estuarine, Coastal and Shelf Science 208:23–35

DeLaune RD, Pezeshki SR, Jugsujinda A (2005) Impact of Mississippi River freshwater reintroduction on Spartina patens marshes: responses to nutrient input and lowering of salinity. Wetlands 25(1):155–161

Holm GO Jr, Perez BC, McWhorter DE, Krauss KW, Johnson DJ, Raynie RC, Killebrew CJ (2016) Ecosystem level methane fluxes from tidal freshwater and brackish marshes of the Mississippi River Delta: implications for coastal wetland carbon projects. Wetlands 36:401–413

Ishtiag KS, Troxler TG, Mab-Wotton L, Wilson BJ, Charles SP, Davis SE, Kominoski JS, Rudnick DT, Sklar FH (2022) Modeling net ecosystem carbon balance and loss in coastal wetlands exposed to sea-level rise and saltwater intrusion. Ecological Applications 32:e2702

Janousek CN, Mayo C (2013) Plant responses to increased inundation and salt exposure: interactive effects on tidal marsh productivity. Plant Ecology 214:917–928

Janousek CN, Dugger BD, Drucker BM, Thorne KM (2020) Salinity and inundation effects on productivity of brackish tidal marsh plants in the San Francisco Bay-Delta Estuary. Hydrobiologia 847:4311–4323

Knox SH, Sturtevant C, Matthes JH, Koteen L, Verfaillie J, Baldocchi D (2014) Agricultural peatland restoration: Effects of land-use change on greenhouse gas (CO_2 and CH_4) fluxes in the Sacramento-San Joaquin Delta. Global Change Biology 21(2):750–765

Krauss KW, Holm GO Jr, Perez BC, McWhorter DE, Cormier N, Moss RF et al (2016) Component greenhouse gas fluxes and radiative balance from two deltaic marshes in Louisiana: pairing chamber techniques and eddy covariance. Journal of Geophysical Research: Biogeosciences 121:1503–1521

Krauss KW, Noe GB, Duberstein JA, Conner WH, Stagg CL, Cormier N, Jones MC et al (2018) The Role of the Upper Tidal Estuary in Wetland Blue Carbon Storage and Flux. Global Biogeochemical Cycles 32:817–839

Lane RR, Mack SK, Day JW, DeLaune RD, Madison MJ, Precht PR (2016) Fate of soil organic carbon during wetland loss. Wetlands 36:1167–1181

Li C, Aber J, Stang F, Butter-Bahl K, Papen H (2000) A process-oriented model of N_2O and NO emissions from forest soils. 1. Model development. Journal of Geophysical Research: Atmospheres 105:4369–4384

Li C, Cui J, Sun G, Trettin CC (2004) Modeling impacts of Management on Carbon Sequestration and Trace Gas Emissions in Forested Wetland Ecosystems. Environmental Management (Supplement) 33:S176-186

Li S, Guo H, Ge Z, Wang D, Liu W, Xie L et al (2020) Sea-level rise will reduce net CO_2 uptake in subtropical coastal marshes. Science of the Total Environment 747:141214

Louisiana Coastal Protection and Restoration Authority (CPRA) (2017) Louisiana's Comprehensive Master Plan for a Sustainable Coast.

https://coastal.la.gov/wp-content/uploads/2017/04/2017-Coastal-Master-Plan_Web-Book_CFinal-with-Effective-Date-06092017.pdf. Accessed 23 Mar 2024

Lu Y, Huang Y, Jia Q, Xie Y (2024) Capturing the net ecosystem CO_2 exchange dynamics of tidal wetlands with high spatiotemporal resolution by integrating process-based and machine learning estimations. Agricultural and Forest Meteorology 352:110045. https://doi.org/10.1016/j.agrformet.2024.110045

Luo M, Huang J, Zhu W, Tong C (2019) Impacts of increasing salinity and inundation on rates and pathways of organic carbon mineralization in tidal wetlands: A Review. Hydrobiologia 827:31–49

Matzke S, Elsey-Quirk T (2018) *Spartina patens* productivity and soil Organic matter response to sedimentation and nutrient enrichment. Wetlands 38:1233–1244

Mayen J, Polsenaere P, Lamaud E, Arnaud M, Kostyrka P, Bonnefond J et al (2024) Atmospheric CO2 exchanges measured by eddy covariance over a temperate salt marsh and influence of environmental controlling factors. Biogeosciences 21:993–1016

Murray NJ, Worthington TA, Bunting P, Duce S, Hagger V, Lovelock CE et al (2022) High-resolution mapping of losses and gains of Earth's tidal wetlands. Science 376(6594):744–749

Neubauer SC, Megonigal JP (2015) Moving beyond global warming potentials to quantify the climatic role of ecosystems. Ecosystems 18(6):1000–1013

Nyman JA, DeLaune RD (1991) CO_2 emission and soil Eh responses to different hydrological conditions in fresh, brackish, and saline marsh soils. Limnology and Oceanography 36(7):1406–1414

Nyman JA, Reid CS, Sasser CE, Linscombe J, Hartley SB, Couvillion BR, Villani RK (2022) Vegetation Types in Coastal Louisiana in 2021 (ver. 2.0, April 2023): US Geological Survey data release. https://doi.org/10.5066/P9URYLMS

Poffenbarger HJ, Needelman BA, Megonigal JP (2011) Salinity influence on methane emissions from tidal marshes. Wetlands 31:831–842

Reichstein M et al (2005) On the separation of net ecosystem exchange into assimilation and ecosystem respiration: Review and improved algorithm. Global Change Biology 11(9):1424–1439

Russell SJ, Windham-Myers L, Stuart-Haëntjens EJ, Bergamaschi BA, Anderson F, Oikawa P, Knox SH (2023) Increased salinity decreases annual gross primary productivity at a Northern California brackish tidal marsh. Environmental Research Letters 18:034045

Sasser CE, Visser JM, Mouton E, Linscombe J, and Hartley SB (2014) Vegetation types in coastal Louisiana in 2013: U.S. Geological Survey Scientific Investigations Map 3290, 1 sheet, scale 1:550,000. https://doi.org/10.3133/sim3290

Saunois M, Stavert AR, Poulter B, Bousquet P, Canadell JG, Jackson RB et al (2020) The global methane budget 2000–2017. Earth System Science Data 12:1561–1623

Snedden GA (2018) Patterning emergent marsh vegetation assemblages in coastal Louisiana, USA, with unsupervised artificial neural networks. Applied Vegetation Science 22:213–229

Snedden GA, Cretini K, Patton B (2015) Inundation and salinity impacts to above- and belowground productivity in *Spartina patens* and *Spartina alterniflora* in the Mississippi River deltaic plain: Implications for using river diversions as restoration tools. Ecological Engineering 81:133–139

Stagg CL, Sharp LA, Fromenthal E, Couvillion B, Woltz V, Piazza S (2024) Accelerating elevation gain indicates land loss associated with erosion in Mississippi River Deltaic Plain tidal wetlands. Estuaries and Coasts. https://doi.org/10.1007/s12237-023-01321-8

Thornton MM, Shrestha R, Wei Y, Thornton PE, Kao S, Wilson BE (2020) Daymet: Daily Surface Weather Data on a 1-km Grid for North America, Version 4. ORNL DAAC, Oak Ridge, Tennessee, USA. https://doi.org/10.3334/ORNLDAAC/1840

Wang H, Hsieh YP, Harwell MA, Huang W (2007) Modeling soil salinity distribution along topographic gradients in tidal salt marshes in Atlantic and Gulf coastal regions. Ecological Modeling 201:429–439

Wang H, Steyer GD, Couvillion BR, Beck HJ, Rybczyk JM, Rivera-Monroy VH, Krauss KW, Visser JM (2017) Predicting landscape effects of Mississippi River diversions on soil organic carbon sequestration. Ecosphere 8(11):e01984. https://doi.org/10.1002/ecs2.1984

Wang H, Krauss KW, Noe GB, Stagg CL, Swarzenski CM, Duberstein JA, Conner WH, DeAngelis DL (2020) Modeling soil porewater salinity response to drought in tidal freshwater forested wetlands. Journal of Geophysical Research: Biogeosciences 125:e2018JG004996

Wang H, Dai Z, Trettin CC, Krauss KW, Noe GB, Burton AJ, Stagg CL, Ward EJ (2022) Modeling impacts of drought-induced salinity intrusion on carbon fluxes and storage in tidal freshwater wetlands. Ecol Appl. https://doi.org/10.1002/eap.2700

Wang H, Dai Z, Trettin CC, Krauss KW, Noe GB, Burton AJ, Ward EJ (2023a) Modeling impacts of saltwater intrusion on methane and nitrous oxide emissions in tidal forested wetlands. Ecol Appl. https://doi.org/10.1002/eap.2858

Wang H, Krauss KW, Noe GB, Dai Z, Trettin CC (2023b) Soil salinity and water level interact to generate tipping points in low salinity tidal wetlands responding to climate change. Estuaries and Coasts. https://doi.org/10.1007/s12237-023-01243-5

Weston NB, Neubauer SC, Velinsky DJ, Vile MA (2014) Net ecosystem carbon exchange and the greenhouse gas balance of tidal marshes along an estuarine salinity gradient. Biogeochemistry 120:163–189

Wilson BJ, Mortazavi B, Kiene RP (2015) Spatial and temporal variability in carbon dioxide and methane exchange at three coastal marshes along a salinity gradient in a northern Gulf of Mexico estuary. Biogeochemistry 123:329–347

Wilson BJ, Servais S, Mazzei V, Kominoski JS, Hu M, Davis SE et al (2018a) Salinity pulses interact with seasonal dry-down to increase ecosystem carbon loss in marshes of the Florida Everglades. Ecological Applications 28(8):2092–2108

Wilson BJ, Servais S, Charles SP, Davis SE, Gaiser E, Kominoski JS, Richards J, Troxler TG (2018b) Declines in plant productivity drive carbon loss from brackish coastal wetland mesocosms exposed to saltwater intrusion. Estuaries and Coasts 41:2147–2158

Zhang Y, Li C, Trettin C, Li H, Sun G (2002) An integrated model of soil, hydrology and vegetation for carbon dynamics in wetland ecosystems. Global Biogeochemical Cycles 16:1–17

Zhu C, Langley JA, Ziska LH, Cahoon DR, Megonigal JP (2022) Accelerated sea-level rise is suppressing CO2 stimulation of tidal marsh productivity: A 33-year study. Science Advances 8:eabn0054